33. Exoskeletons for Human Performance Augmentation

Homayoon Kazerooni

Although autonomous robotic systems perform remarkably in structured environments (e.g., factories), integrated human–robotic systems are superior to any autonomous robotic systems in unstructured environments that demand significant adaptation. The technology associated with exoskeleton systems and human power augmentation can be divided into lower-extremity exoskeletons and upper-extremity exoskeletons. The reason for this was twofold; firstly, one could envision a great many applications for either a stand-alone lower- or upper-extremity exoskeleton in the immediate future. Secondly, and more importantly for the division, is that these exoskeletons are in their early stages, and further research still needs to be conducted to ensure that the upper-extremity exoskeleton and lower-extremity exoskeleton can function well independently before one can venture an attempt to integrate them. This chapter first gives a description of the upper-extremity exoskeleton efforts and then will proceed with the more detailed description of the lower-extremity exoskeleton.

33.1 Survey of Exoskeleton Systems 773
33.2 Upper-Extremity Exoskeleton 775
33.3 Intelligent Assist Device 776
33.4 Control Architecture for Upper-Extremity Exoskeleton Augmentation 778
33.5 Applications of Intelligent Assist Device .. 780
33.6 Lower-Extremity Exoskeleton 780
33.7 The Control Scheme of an Exoskeleton 782
33.8 Highlights of the Lower-Extremity Design 786
33.9 Field-Ready Exoskeleton Systems 790
33.9.1 The ExoHiker Exoskeleton 790
33.9.2 The ExoClimber Exoskeleton 790
33.10 Conclusion and Further Reading 792
References 792

33.1 Survey of Exoskeleton Systems

In the early 1960s, the US Defense Department expressed interest in the development of a man-amplifier, a *powered suit of armor* which would augment soldiers' lifting and carrying capabilities. In 1962, the Air Force had the Cornell Aeronautical Laboratory study the feasibility of using a master–slave robotic system as a man-amplifier. In later work, Cornell determined that an exoskeleton, an external structure in the shape of the human body which has far fewer degrees of freedom than a human, could accomplish most desired tasks [33.1]. From 1960 to 1971, General Electric developed and tested a prototype man-amplifier, a master–slave system called the Hardiman [33.2–6]. The Hardiman was a set of overlapping exoskeletons worn by a human operator. The outer exoskeleton (the slave) followed the motions of the inner exoskeleton (the master), which followed the motions of the human operator. All these studies found that duplicating all human motions and using master–slave systems were not practical. Additionally, difficulties in human sensing and system complexity kept it from walking.

Vukobratovic et al. developed a few active orthoses for paraplegics [33.7]. The systems include hydraulic or pneumatic actuators for driving the hip and knee joints in the sagittal plane. These orthoses were coupled with the wearer via shoe bindings, cuffs, and a corset. The device was externally powered and controlled via a predetermined periodic motion. Although these early devices

were limited to predefined motions and had limited success, balancing algorithms developed for them are still used in many bipedal robots [33.8].

Seireg et al. also created an exoskeleton system for paraplegics where only the hip and knee were powered by hydraulic actuators in sagittal plane [33.9]. The hydraulic power unit consists of a battery-powered direct-current (DC) motor, pump, and accumulator. A bank of servo-valves drives the actuators at the knee and hip. The device was controlled to follow a set of joint trajectories without the use of any sensory systems from its wearer.

The hybrid assisted limb (HAL) was developed at the University of Tsukuba ([33.13, 14]). This 15 kg battery-powered suit detects muscle myoelectrical signals on the skin surface below the hip and above the knee. The signals are picked up by the sensors and sent to the computer, which translates the nerve signals into signals of its own for controlling electric motors at the hips and knees of the exoskeleton, effectively amplify-

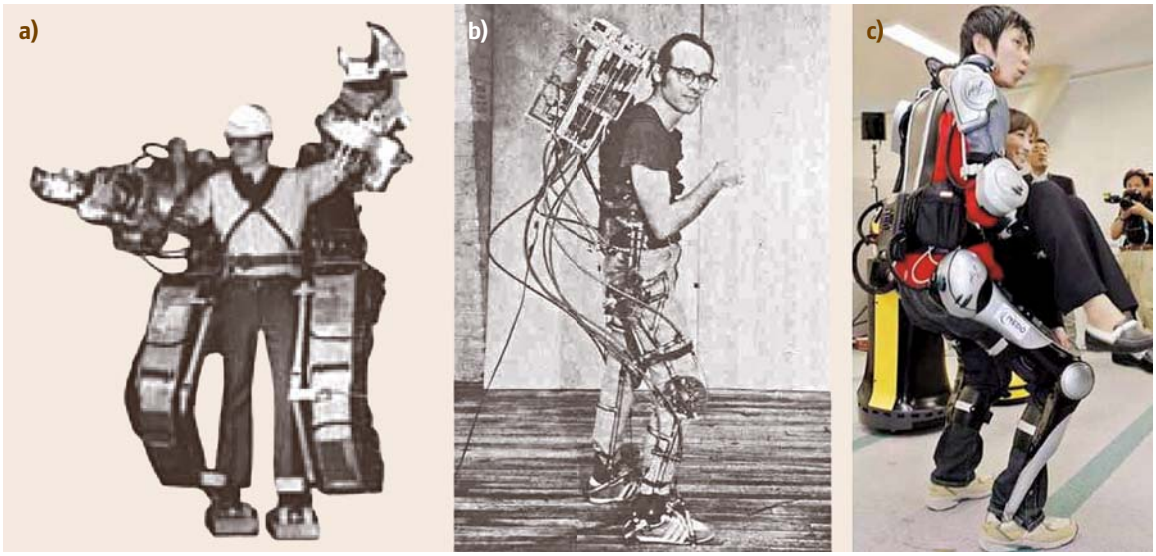

Fig. 33.1 (a) Hardiman; (b) An exoskeleton system designed for paraplegics by *Seireg* et al. [33.9]; (c) HAL

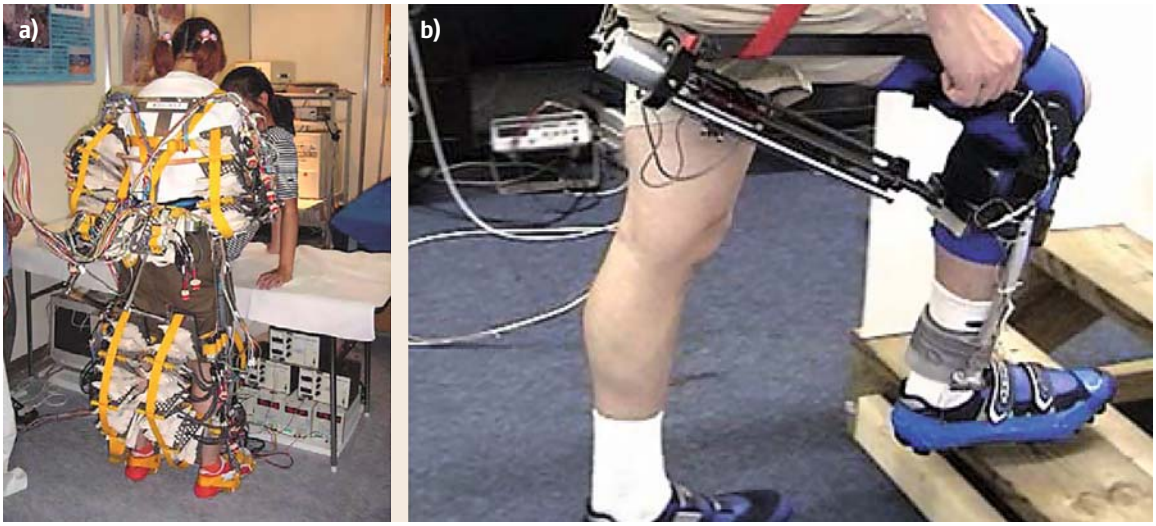

Fig. 33.2 (a) An exoskeleton for patient handling [33.10, 11]; (b) RoboKnee [33.12]

ing muscle strength. In addition to electromyography (EMG) signals, the device further includes potentiometers for measuring the joint angles, force sensors for measuring the ground reaction forces and a gyroscope and accelerometer for measuring the torso angle. Each leg of HAL powers the flexion/extension motion at the hip and knee in the sagittal plane through the use of DC motors integrated with harmonic drives. The ankle includes passive degrees of freedom.

Yamamoto et al. [33.10, 11] have created an exoskeleton system for assisting nurses during patient handling. The lower limbs include pneumatic actuators for the flexion/extension of the hips and knees in the sagittal plane. Air pumps are mounted directly onto each actuator to provide pneumatic power. User input is determined via force sensing resistors coupled to the wearer's skin. The measurement from force sensing resistor (FSR) and other information such as joint angles are used to determine the required input torques for various joints.

Pratt et al. developed a powered knee brace for adding power at the knee to assist in squatting [33.12]. The device is powered by a linear series-elastic actuator coupling the upper and the lower portions of a knee brace. The control of this powered knee brace requires the ground reaction force measured by two load cells. The system uses a positive-feedback force controller to create an appropriate force for the actuator.

Kong et al. developed a full lower-limb exoskeleton system that works with a powered walker [33.15]. The walker houses the electric actuators, the controller, and the batteries, reducing the weight of the exoskeleton system. A transmission system transmits power to the wearer's joints from the actuators in the walker. The exoskeleton is powered at the hips and knees in sagittal plane. The input to drive the system is a set of pressure sensor that measure the force applied by the quadriceps muscle on the knee.

Agrawal et al. have conducted research projects on statically balanced leg orthoses that allow for less effort during swing [33.16]. In the passive version, the device uses springs in order to cancel the gravity force associated with the device links and the person leg. Through experiments the authors showed that the device reduced the required torque by the wearer substantially.

33.2 Upper-Extremity Exoskeleton

In the mid-1980s, researchers at Berkeley initiated several research projects on upper-extremity exoskeleton systems, billed as *human extenders* [33.17–23]. The main function of an upper-extremity exoskeleton is human power augmentation for the manipulation of heavy and bulky objects. Since upper-extremity exoskeletons are mostly used for factory floors, warehouse, and distribution centers, they are hung from overhead cranes. As can be seen in later sections, lower-extremity exoskeletons focus on supporting and carrying heavy payloads on the operator's back (like a backpack) during long-distance locomotion. Upper-extremity exoskeletons, which are also known as assist devices or human power extenders, can simulate forces on a worker's arms and torso. These forces differ from, and are usually much smaller than the forces needed to maneuver a load. When a worker uses an upper-extremity exoskeleton to move a load, the device bears the bulk of the weight by itself, while transferring to the user as a natural feedback a scaled-down value of the load's actual weight. For example, for every 20 kg of weight from an object, a worker might support only 2 kg while the device supports the remaining 18 kg. In this fashion, the worker can still sense the load's weight and judge his/her movements accordingly, but the force he/she feels is much smaller than what he/she would feel without the device. In another example, suppose the worker uses the device to maneuver a large, rigid, and bulky object, such as an exhaust pipe. The device will convey the force to the worker as if it was a light, single-point mass. This limits the cross-coupled and centrifugal forces that increase the difficulty of maneuvering a rigid body and can sometimes produce injurious forces on the wrist. In a third example, suppose a worker uses the device to handle a powered torque wrench. The device will decrease and filter the forces transferred from the wrench to the worker's arm so the worker feels the low-frequency components of the wrench's vibratory forces instead of the high-frequency components that produce fatigue [33.24]. These assist devices not only filter out unwanted forces on a worker, but can also be programmed to follow a particular trajectory regardless of the exact direction in which the worker attempts to manipulate the device. For example, suppose an auto-assembly worker is using an assist device to move a seat to its final destination inside a car. The assist device can bring the seat to its final destination, moving it along a preprogrammed path with a speed that is proportional

Fig. 33.3a,b Two-handed upper-extremity exoskeleton where artificially built friction forces between the load and the arms allow for grasping objects [33.25]

to the magnitude of the worker's force on the device. Although the worker might be paying very little attention to the final destination of the seat, the device can still bring the seat to its proper place without the worker's guidance. The upper-extremity exoskeleton reflects on the worker's arm forces that are limited and much smaller than the forces needed to maneuver loads. With it, autoassembly and warehouse workers can maneuver parts and boxes with greatly improved dexterity and precision, not to mention a marked decrease in muscle strain.

Fig. 33.4 One-handed upper-extremity exoskeleton where a griper allows for grasping of heavy objects [33.21]

The upper-extremity exoskeleton will significantly reduce the incidence of back injury in the workplace, which will in turn greatly decrease the annual cost of treating back injuries.

Upper-extremity exoskeletons were designed based primarily on compliance control [33.26–29] schemes that relied on the measurement of interaction force between the human and the machine. Various experimental systems, including a hydraulic loader designed for loading aircrafts and an electric power extender built for two-handed operation, were designed to verify the theories (Fig. 33.3 and Fig. 33.4).

33.3 Intelligent Assist Device

The intelligent assist devices (IAD) are the simplest non-anthropomorphic form of the upper-extremity systems that augments human capabilities [33.30, 31]. Figure 33.5 illustrates an intelligent assist device (IAD). At the top of the device, a computer-controlled electric actuator is attached directly to a ceiling, wall, or an overhead crane and moves a strong wire rope precisely, and with a controllable speed. Attached to the wire rope is a sensory end-effector where the operator hand, the IAD, and the load come into contact. The end-effector includes a load interface subsystem and an operator interface subsystem. The load interface subsystem is designed to interface with a variety of loads and holding devices. Hooks, suction cups, and grippers are examples of other connections to the end-effector as shown in Fig. 33.6. In general, to grab complex objects, special tooling systems should be made and connected to the load interface subsystem. The operator interface subsystem includes an ergonomic handle, which contains a high-performance sensor for measuring the magnitude of the vertical force exerted on the handle by the operator. A signal representing the operator force is transmitted to a computer controller, which controls the actuator of the IAD. Using the measurement of the operator force and other calculations, the controller assigns the necessary speed to either raise or lower the wire rope to create enough mechanical strength to assist the operator in the lifting task as required. If the operator pushes upwardly on the handle, the assist device lifts the load; and if the operator pushes downward on the handle, the assist device lowers the load. The load moves appropriately so that only a small preprogrammed proportion of the load force (weight plus acceleration) is supported by the operator, and the remaining force is provided by the actuator of the IAD. All of this happens so quickly that the operator's lifting efforts and the device's lifting efforts are

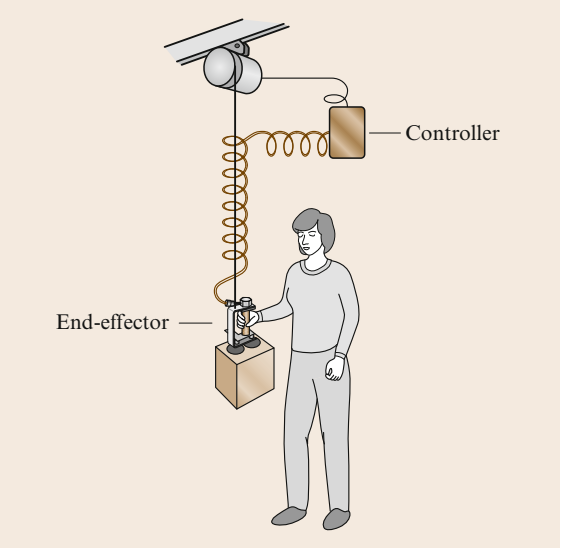

Fig. 33.5 Intelligent assist device: the simplest form of upper-extremity enhancers for industrial applications. The IAD can follow a worker's high-speed maneuvers very closely during manipulations without impeding the worker's motion.

synchronized perfectly and the load feels substantially lighter to the operator. With this load-sharing concept, the operator has the sense that he or she is lifting the load, but with far less force than would ordinarily be required. For example, with a 25 kg load force (gravity plus acceleration), the IAD supports 24 kg, while the operator supports and feels only 1 kg. With the assistance of the intelligent assist device, a worker can manipulate any object in the same natural way that he/she would manipulate a lightweight object without any assistance. There are no push buttons, keyboards, switches, or valves to control the motion of the intelligent assist device; the user's natural movements, in conjunction with the device computer, controls the motion of the device and its load.

Figure 33.6 shows the end-effector that measures the operator forces at all times even in the presence of loading and unloading shock forces. This robust end-effector also includes a dead-man switch, which is installed on the handle and sends a signal to the controller via a signal cable. If the dead-man switch on the end-effector is not depressed, (i. e., if the operator is not holding onto the handle of the end-effector), the device will be suspended without any motion even if loads are added to or removed from the end-effector.

The IAD is engineered with variety of embedded safety features. One of the most important safety characteristics of the IAD is that the wire rope does not become slack if the end-effector is physically constrained from moving downward and the end-effector is pushed downward by the operator. Slack in the wire rope can have far more serious consequences than slowing down the workers at their jobs; the slack line could wrap around the operator's neck or hand, creating serious or even deadly injuries. The control algorithm in the computer of the IAD, employing the information from various sensors, ensures that the wire rope will never become slack [33.32].

Another form of IAD can be seen in Fig. 33.7 where a sensory glove measures the force the wearer imposes

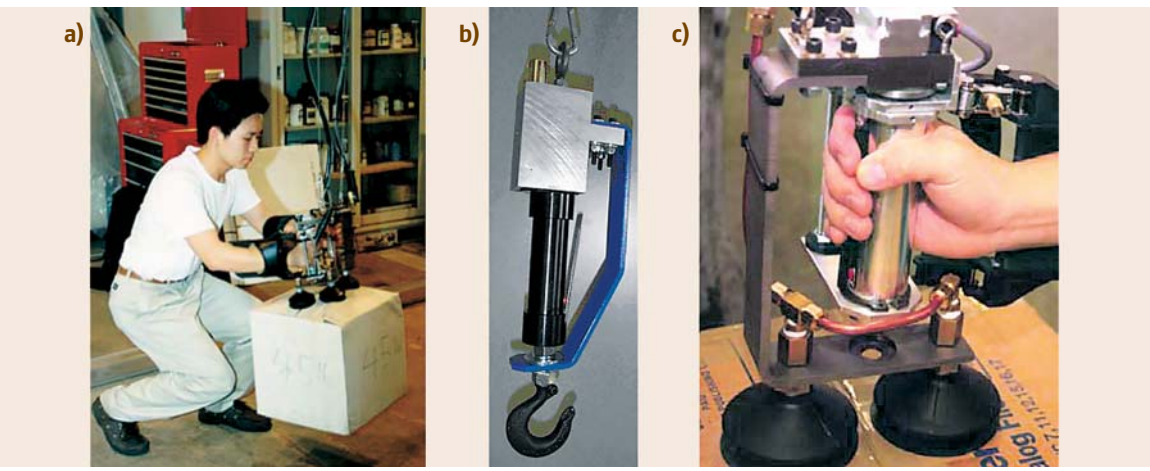

Fig. 33.6a–c The end-effector (**a**) contains a sensor (**b**) that measures the force that the operator applies to the handle (**c**) in the vertical direction

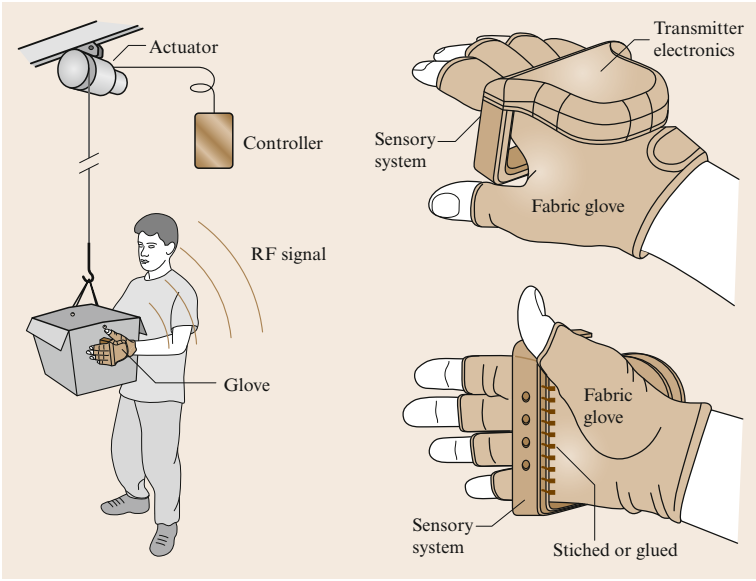

Fig. 33.7 An instrumented glove allows an operator to lift and lower objects naturally while using a hoist, similar to the way one maneuvers objects manually without activating switches or push buttons [33.34]

on any part of the material handling system or the object being maneuvered [33.33, 34]. This instrumented glove is always worn by the operator and therefore remains with the operator. The instrumented glove generates a set of signals as a function of the contact force between the glove and the object being manipulated or the material handling device itself. A set of signals representing the contact force is transmitted in the form of radiofrequency (RF) signals to a device controller so that a command signal is generated. The command signal is sent to the device actuator to provide the required assistance to maneuver or lift the load as a function of the force imposed by the operator, so that the operator provides only a small portion of the total force needed to maneuver the device and the object being manipulated by the device. For a person observing the operator and the IAD, this interaction seems rather magical since the device responds to the operator's touch regardless of whether the operator is pushing on the IAD or on the object being lifted by the device.

33.4 Control Architecture for Upper-Extremity Exoskeleton Augmentation

The linear system theory is employed here to model the dynamic behavior of the elements of an IAD. This allows us to disclose the system properties in their simplest and most commonly used form. The more general approach (nonlinear and multivariable models for upper-extremity assist devices) are presented in [33.19, 20], and [33.21], where they have been applied to the devices shown in Figs. 33.3 and 33.4. The block diagram of Fig. 33.8 shows the basic control technique. As discussed earlier, the force-sensing element in the end-effector delivers a signal to the controller, which is used to control the actuator. If e is the input command to the actuator, then the linear velocity of the end-effector v can be represented by:

$$v = Ge + Sf_{\mathrm{R}} \,, \tag{33.1}$$

where G is the actuator transfer function relating the input command to the actuator to the end-effector velocity; S is the actuator sensitivity transfer function relating the wire rope tensile force f_{R} to the end-effector velocity, v. A positive value for v represents a downward speed for the load. Also note that, since the load is connected to the end-effector, both terminologies *load velocity* and *end-effector velocity* refer to v as derived by (33.1). If a closed-loop velocity controller is designed for the actuator such that S is small, the actuator has only a small response to the line tensile

force. A high-gain controller in the closed-loop velocity system results in a small S and consequently a small change in velocity v in response to the line tensile force. Also note that non-back-drivable speed reducers (usually high transmission ratios) produce a small S for the system.

The rope tensile force f_R can be represented by:

$$f_R = f + p\,, \tag{33.2}$$

where f is the operator-applied force on the end-effector; the force p imposed by the load and the end-effector is referred to herein as the *load force* on the line. Positive values for f and p represent downward forces. Note that p is the force imposed on the line and is equal to the weight and inertia force of the load and end-effector taken together:

$$p = W - \frac{W}{g}\frac{\mathrm{d}}{\mathrm{d}t}v\,, \tag{33.3}$$

where W is the weight of the end-effector and load taken together as a whole and $\frac{\mathrm{d}}{\mathrm{d}t}v$ is the acceleration of the end-effector and load. If the load does not have any acceleration or deceleration, then p is exactly equal to the weight of the end-effector and load W. The operator force f is measured and passed to the controller delivering the output signal e. A positive number f_0 in the computer is subtracted from the measurement of the human force f. The role of f_0 is explained later. If the transfer function of the controller is represented by K, then the output of the controller e is:

$$e = K(f - f_0)\,. \tag{33.4}$$

Substituting for f_R and e from (33.2) and (33.4) into (33.1) results in the following equation for the end-effector velocity v:

$$v = GK(f - f_0) + S(f + p)\,. \tag{33.5}$$

Measuring an upward human force on the end-effector or on the load is only possible when the line is under tension from the weight of the end-effector. If the end-effector is light, then the full range of human upward forces may be neglected by the sensor in the instrumented glove. To overcome this problem, a positive number f_0 is introduced into (33.4). As (33.5) shows, the absence of f and p will cause the end-effector to move upwardly. Suppose the maximum downward force imposed by the operator is f_{max}. Then f_0 is preferably set at approximately half of f_{max}. Substituting for f_0 in (33.5), (33.6) represents the load velocity:

$$v = GK\left(f - \frac{f_{max}}{2}\right) + S(f + P)\,. \tag{33.6}$$

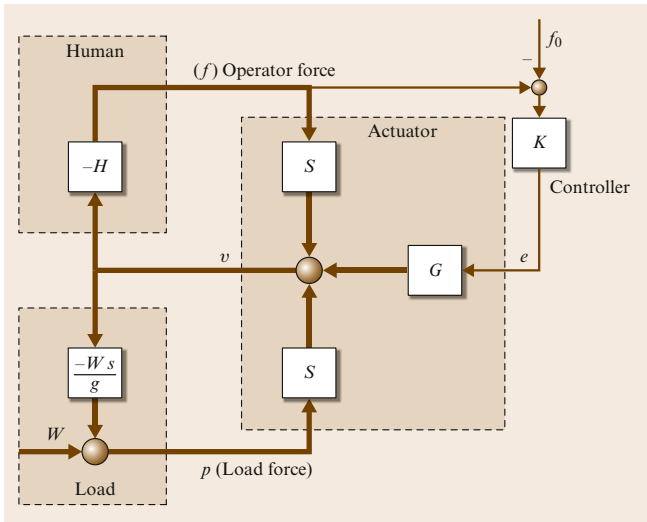

Fig. 33.8 The control block diagram of an intelligent assist device

If the operator pushes downward such that $f = f_{max}$, then the maximum downward velocity of the load is:

$$v_{down} = GK\left(\frac{f_{max}}{2}\right) + S(f + P)\,. \tag{33.7}$$

If the operator does not push at all, then the maximum upward velocity of the end-effector or the load is:

$$v = -GK\left(\frac{f_{max}}{2}\right) + S(f + P)\,. \tag{33.8}$$

Therefore, by the introduction of f_0 in (33.4), one need not be concerned about the measurement of the upward human force. If $S = 0$, the upward and downward maximum speeds are identical in magnitude. However, in the presence of nonzero S, for a given load and under equal conditions, the magnitude of the maximum upward speed is smaller than the magnitude of the maximum downward speed. This is very natural and intuitive for the operator. Going back to (33.5), it can be observed that the more force an operator imposes on the load or on the line, the larger the velocity of the load and end-effector will be. Using the measurement of the operator force, the controller assigns the proper pulley speed to create sufficient mechanical strength, in order to assist the operator in the lifting task. In this way, the end-effector follows the human arm motions naturally. Equation (33.5) suggests that, when the operator increases or decreases the downward force on an object, a corresponding increase or decrease occurs in the downward speed of the object. Alternatively, an increase or decrease in the object's weight causes a decrease or increase, respectively, in the

upward object speed for a given operator force on the object. As Fig. 33.8 indicates, K may not be arbitrarily large. Rather, the choice of K must guarantee the closed-loop stability of the system. The human force f is a function of the human arm impedance H, whereas the load force is a function of load dynamics, i. e., the weight and inertial forces generated by the load. One can find many methods to design the controller transfer function K. Reference [33.19] describes the conditions for the closed-loop stability of such systems.

33.5 Applications of Intelligent Assist Device

The IAD was designed with one vision in mind: minimizing the risk of injuries associated with repeated maneuvers, and maximizing the throughput while maintaining robustness and user-friendliness. The IAD has been evaluated extensively for three applications: warehousing and distribution centers, auto-assembly plants, and delivery services. A study on warehousing maneuvers at distribution centers demonstrated that palletizing, depalletizing, loading and unloading trucks, and placing boxes on and off of conveyor belts are the most common maneuvers. Initial studies of the distribution centers demonstrated that objects to be maneuvered in warehouses and distribution centers are mostly boxes weighing less than 27 kg that require workers to maneuver them rapidly (sometimes up to 15 boxes a minute). The use of the IADs in warehouses would have a considerable impact on reducing injuries to the worker population because of the large number of warehouse workers. Figure 33.6 shows the use of the IAD in a distribution center during a depalletizing operation.

Studies of auto-assembly maneuvers revealed that the installation of batteries, gas tanks, bumpers, instrument panels, exhaust pipes, and prop shafts are important maneuvers that would benefit from IADs (Fig. 33.9). Various load interface subsystems must be employed for connection to various auto parts.

Postal services across the world use sacks and trays to hold letters, magazines, and small boxes. These sacks and trays, which are manually handled by mail handlers, are usually fully filled with magazine bundles, envelopes and parcels, and can weigh up to 32 kg. In general, at all distribution centers, several factors contribute to the creation of awkward and uncomfortable handling situations for mail handlers:

Fig. 33.9a,b The use of IADs for mail and package delivery service **(a)** and automobile industries **(b)**

- the heavy weight of the sacks and letter trays and letter tubs
- the lack of handles, eyelets or any other helpful operator interface on the sacks and parcels
- the unpredictable shape, size, and weight of the sacks and letter trays and letter tubs at a work station

Intelligent assist devices greatly reduce the risk of back injuries when used by workers performing repetitive maneuvers. This reduction in injury, in turn, will greatly reduce the national cost of treating back injuries. See [33.35] and [33.36] for end-effectors that are deigned for grasping postal sacks.

33.6 Lower-Extremity Exoskeleton

The first field-operational lower-extremity exoskeleton (commonly referred to as BLEEX) is comprised of two powered anthropomorphic legs, a power unit, and a backpack-like frame on which a variety of heavy loads can be mounted. This system provides its pilot (i. e., the wearer) with the ability to carry significant loads

on his/her back with minimal effort over any type of terrain. BLEEX allows the pilot to comfortably squat, bend, swing from side to side, twist, and walk on ascending and descending slopes, while also offering the ability to step over and under obstructions while carrying equipment and supplies. Because the pilot can carry significant loads for extended periods of time without reducing his/her agility, physical effectiveness increases significantly with the aid of this class of lower-extremity exoskeletons. In order to address issues of field robustness and reliability, BLEEX is designed such that, in the case of power loss (e.g., from fuel exhaustion), the exoskeleton legs can be easily removed and the remainder of the device can be carried like a standard backpack.

BLEEX was first unveiled in 2004, at UC Berkeley's Human Engineering and Robotics Laboratory. In this initial model, BLEEX offered a carrying capacity of 34 kg (75 lbs), with weight in excess of that allowance being supported by the pilot. BLEEX's unique design offers an ergonomic, highly maneuverable, mechanically robust, lightweight, and durable outfit to surpass typical human limitations. BLEEX has numerous potential applications; it can provide soldiers, disaster relief workers, wildfire fighters, and other emergency personnel with the ability to carry heavy loads such as food, rescue equipment, first-aid supplies, communications gear, and weaponry, without the strain typically associated with demanding labor. Unlike unrealistic fantasy-type concepts fueled by movie-makers and science-fiction writers, the lower-extremity exoskeleton conceived at Berkeley is a practical, intelligent, load-carrying robotic device. It is our vision that BLEEX will provide a versatile and realizable transport platform for mission-critical equipment.

Fig. 33.10 Berkeley lower-extremity exoskeleton (BLEEX) and pilot Ryan Steger. 1: The load occupies the upper portion of the backpack and around the power unit; 2: rigid connection of the BLEEX spine to the pilot's vest; 3: the power unit and central computer occupies the lower portion of the backpack; 4: semirigid vest connecting BLEEX to the pilot; 5: one of the hydraulic actuators; 6: rigid connection of the BLEEX feet to the pilot's boots

The effectiveness of the lower-extremity exoskeleton stems from the combined benefit of the human intellect provided by the pilot and the strength advantage offered by the exoskeleton; in other words, the human provides an intelligent control system for the exoskeleton while the exoskeleton actuators provide most of the strength necessary for walking. The control algorithm ensures that the exoskeleton moves in concert with the pilot with minimal interaction force between the two. The control scheme needs no direct measurements from the pilot or the human–machine interface (e.g., no force sensors between the two); instead, the controller estimates, based on measurements from the exoskeleton only, how to move so that the pilot feels very little force. This control scheme, which has never before been applied to any robotic system, is an effective method of generating locomotion when the contact location between the pilot and the exoskeleton is unknown and unpredictable (i. e., the exoskeleton and the pilot are in contact in variety of places). This control method differs from compliance control methods [33.27,28] employed for upper-extremity exoskeletons [33.17,21] and haptic systems [33.18, 19] because it requires no force sensor between the wearer and the exoskeleton.

The basic principle for the control of an exoskeleton rests on the notion that the exoskeleton needs to shadow the wearer's voluntary and involuntary movements quickly, and without delay. This requires a high level of sensitivity in response to all forces and torques on the exoskeleton, particularly the forces imposed by the pilot. Addressing this need involves a direct conflict with control science's goal of minimizing system sensitivity in the design of a closed-loop feedback system. If fitted with a low sensitivity, the exoskeleton would not move in concert with its wearer. One should realize, however, that maximizing system sensitivity to external forces and torques leads to a loss of robustness in the system.

Taking into account this new approach, the goal is to develop a controller for the exoskeleton with high sensitivity. One is faced with two realistic concerns; the first was that an exoskeleton with high sensitivity to external forces and torques would respond to other external forces not initiated by its pilot, for example, if someone pushed against an exoskeleton that had high sensitivity, the exoskeleton would move just as it would in response to forces from its pilot. Although the fact that it does not stabilize its behavior on its own in response to other forces may sound like a serious problem, if it did (e.g., using a gyro) the pilot would receive motion from the exoskeleton unexpectedly and would have to struggle with it to avoid unwanted movement. The key to stabilizing the exoskeleton and preventing it from falling in response to external forces depends on the pilot's ability to move quickly (e.g., step back or sideways) to create a stable situation for himself and the exoskeleton. For this, a very wide control bandwidth is needed so that the exoskeleton can respond to both pilot's voluntary and involuntary movements (i. e., reflexes).

The second concern is that systems with high sensitivity to external forces and torques are not robust to variations and therefore the precision of the system performance will be proportional to the precision of the exoskeleton dynamic model. Various experimental systems in Berkeley have proved the overall effectiveness of the control method in shadowing the pilot's movement.

33.7 The Control Scheme of an Exoskeleton

The control of the exoskeleton is motivated here through the simple one-degree-of-freedom (1-DOF) example shown in Fig. 33.11. This figure schematically depicts a human leg attached or interacting with a 1-DOF exoskeleton leg in a swing configuration (no interaction with the ground). For simplicity, the exoskeleton leg is shown as a rigid link pivoting about a joint and powered by a single actuator. The exoskeleton leg in this example has an actuator that produces a torque about pivot point A.

Although the pilot is securely attached to the exoskeleton at the foot, other parts of the pilot leg, such as the shanks and thighs, can contact the exoskeleton and impose forces and torques on the exoskeleton leg. The location of the contacts and the direction of the contact forces (and sometimes contact torques) vary and are therefore considered unknown values in this analysis. In fact, one of the primary objectives in designing BLEEX was to ensure a pilot's unrestricted interaction with the exoskeleton. The equivalent torque on the exoskeleton leg, resulting from the pilot's applied forces and torques, is represented by d.

In the absence of gravity, (33.9) and the block diagram of Fig. 33.12 represent the dynamic behavior of the exoskeleton leg regardless of any kind of internal feedback the actuator may have

$$v = Gr + Sd\,, \tag{33.9}$$

where G represents the transfer function from the actuator input r to the exoskeleton angular velocity v (the actuator dynamics are included in G). In the case where multiple actuators produce controlled torques on the system, r is the vector of torques imposed on the exoskeleton by the actuators. The form of G and the type of internal feedback for the actuator is immaterial for the discussion here. Also bear in mind the omission of the Laplace operator in all equations for the sake of compactness.

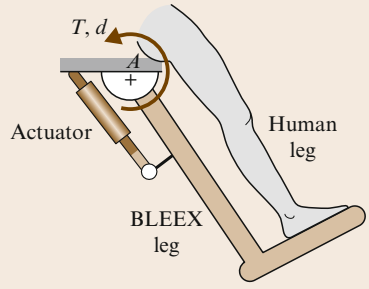

Fig. 33.11 Simple one-DOF exoskeleton leg interacting with the pilot leg. The exoskeleton leg has an actuator that produces a torque T about the pivot point A. The total equivalent torque associated with all forces and torques from the pilot on the exoskeleton is represented by d

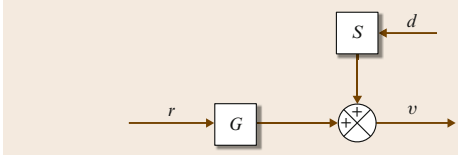

Fig. 33.12 The exoskeleton's angular velocity is shown as a function of the input to the actuators and the torques imposed by the pilot on the exoskeleton

The exoskeleton velocity, as shown by (33.9), is affected by forces and torques from its pilot. The sensitivity transfer function, S, represents how the equivalent human torque affects the exoskeleton angular velocity; S maps the equivalent pilot torque d onto the exoskeleton velocity v. If the actuator already has some sort of primary stabilizing controller, the magnitude of S will be small and the exoskeleton will only have a small response to the imposed forces and torques from the pilot or any other source. For example, a high-gain velocity controller in the actuator results in small S, and consequently a small exoskeleton response to forces and torques. Also, non-back-drivable actuators (e.g., large transmission ratios or servo-valves with overlapping spools) result in a small S, which leads to a correspondingly small response to pilot forces and torques.

Note that d (the resulting torque from pilot on the exoskeleton) is not an exogenous input; it is a function of the pilot dynamics and variables such as position and velocity of the pilot and the exoskeleton legs. These dynamics change from person to person, and within a person as a function of time and posture. It is assumed that d is only from the pilot and does not include any other external forces and torques.

The objective is to increase exoskeleton sensitivity to pilot forces and torques through feedback but without measuring d. Measuring d to create such systems develops several hard, but ultimately solvable, problems in the control of a lower-extremity exoskeleton. Some of those problems are briefly described below.

1. Depending on the architecture and the design of the exoskeleton, one needs to install several force and torque sensors to measure all forces from the pilot on the exoskeleton because the pilot is in contact with the exoskeleton at several locations. These locations are not known in advance. For example, we have found that some pilots are interested in having braces connecting an exoskeleton at the shanks while some are interested in having them on the thighs. Inclusion of sensors on a leg to measure all kinds of human forces and torques may result in a system suitable for a laboratory setting but not robust enough to be deployed in the field.
2. If the exoskeleton design is such that the forces and torques applied by the pilot on the exoskeleton are limited to a specified location (e.g., the pilot foot), the sensor that measures the pilot forces and torques will also inadvertently measure other forces and torques that are not intended for locomotion. This is a major difference between measuring forces from, for example, the human hands, and measuring forces from the human lower limbs. Using our hands, we are able to impose controlled forces and torques on upper extremity exoskeletons and haptic systems with very few uncertainties. However, our lower limbs have other primary and nonvoluntary functions like load support that take priority over locomotion.
3. One option which was experimented with was the installation of sensing devices for forces on the bottom of the pilot's boots, where they are connected to the exoskeleton. Since the force on the bottom of the pilot's boot travels from heel to toe during normal walking, several sensors are required to measure the pilot force. Ideally, one would have a matrix of force sensors between the pilot and exoskeleton feet to measure the pilot forces at all locations and at all directions, though in practice, only a few sensors could be accommodated: at the toe, ball, midfoot, and the heel. Still, this option leads to thick and bulky soles.
4. The bottoms of the human boots experience cyclic forces and torques during normal walking that lead to fatigue and eventual sensor failure if the sensor is not designed and isolated properly.

For the above reasons and our experience in the design of various lower-extremity exoskeletons, it became evident that the existing state of technology in force sensing could not provide robust and repeatable measurement of the human lower limb force on the exoskeleton. Our goal then shifted to developing an exoskeleton with a large sensitivity to forces and torques from the operator using measurements only from the exoskeleton (i. e., no sensors on the pilot or the exoskeleton interface with the pilot). Creating a feedback loop from the exoskeleton variables only, as shown in Fig. 33.13 the new closed-loop sensitivity transfer function is presented in (33.10).

$$S_{\mathrm{NEW}} = \frac{v}{d} = \frac{S}{1+GC} \,. \tag{33.10}$$

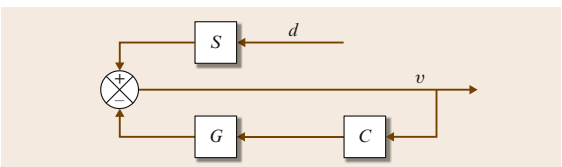

Fig. 33.13 The feedback control loop added to block diagram of Fig. 33.12; C is the controller operating only on the exoskeleton variables

Observation of (33.10) reveals that $S_{NEW} \leq S$, and therefore any negative feedback from the exoskeleton leads to an even smaller sensitivity transfer function. With respect to (33.10), our goal is to design a controller for a given S and G such that the closed-loop response from d to v (the new sensitivity function as given by (33.10)) is greater than the open-loop sensitivity transfer function (i. e., S) within some bounded frequency range. This design specification is given by inequality (33.11)

$$|S_{NEW}| > |S| , \quad \forall\omega \in (0, \omega_0) , \tag{33.11}$$

or alternatively

$$|1 + GC| < 1 \quad \forall\omega \in (0, \omega_0) , \tag{33.12}$$

where ω_0 is the exoskeleton maneuvering bandwidth.

In classical and modern control theory, every effort is made to minimize the sensitivity function of a system to external forces and torques. But for exoskeleton control, one requires a totally opposite goal: *to maximize the sensitivity of the closed-loop system to forces and torques*. In classical servo problems, negative feedback loops with large gains generally lead to small sensitivity within a bandwidth, which means that they reject forces and torques (usually called disturbances). However, the above analysis states that the exoskeleton controller needs a large sensitivity to forces and torques.

To achieve a large sensitivity function, it is suggested that one uses the inverse of the exoskeleton dynamics as a positive feedback controller so that the loop gain for the exoskeleton approaches unity (slightly less than 1). Assuming positive feedback, (33.10) can be written as

$$S_{NEW} = \frac{v}{d} = \frac{S}{1 - GC} . \tag{33.13}$$

If C is chosen to be $C = 0.9G^{-1}$, then the new sensitivity transfer function is $S_{NEW} = 10S$ (ten times the force amplification). In general we recommend the use of positive feedback with a controller chosen as:

$$C(1 - \alpha^{-1})G^{-1} , \tag{33.14}$$

where α is the amplification number greater than unity (for the above example, $\alpha = 10$ led to the choice of $C = 0.9G^{-1}$). Equation (33.14) simply states that a positive-feedback controller needs to be chosen as the inverse dynamics of the system dynamics scaled down by $(1 - \alpha^{-1})$. Note that (33.14) prescribes the controller in the absence of unmodeled high-frequency exoskeleton dynamics. In practice, C also includes a unity-gain low-pass filter to attenuate the unmodeled high-frequency exoskeleton dynamics.

The above method works well if the system model (i. e., G) is well known to the designer. If the model is not well known, then the system performance will differ greatly from the one predicted by (33.13), and in some cases instability will occur. The above simple solution comes with an expensive price: robustness to parameter variations. In order to get the above method working, one needs to know the dynamics of the system well, to understand the dynamics of the exoskeleton quite well, as the controller is heavily model based. One can see this problem as a tradeoff: the design approach described above requires no sensor (e.g., force or EMG) in the interface between the pilot and the exoskeleton; one can push and pull against the exoskeleton in any direction and at any location without measuring any variables on the interface. However, the control method requires a very good model of the system. At this time, the experiments with the exoskeleton have shown that this control scheme – which does not stabilize the exoskeleton – forces the system to follow wide-bandwidth human maneuvers while carrying heavy loads. We have come to believe, to rephrase Friedrich Nietzsche, that *that which does not stabilize, will only make us stronger*. Reference [33.37] describes a system identification method for BLEEX.

How does the pilot dynamic behavior affect the exoskeleton behavior? In our control scheme, there is no need to include the internal components of the pilot limb model; the detailed dynamics of nerve conduction, muscle contraction, and central nervous system processing are implicitly accounted for in constructing the dynamic model of the pilot limbs. The pilot force on the exoskeleton, d, is a function of both the pilot dynamics, H, and the kinematics of the pilot limb (e.g., velocity, position or a combination thereof). In general, H is determined primarily by the physical properties of the human dynamics. Here it is assumed H is a nonlinear operator representing the pilot impedance as a function of the pilot kinematics

$$d = -H(v) . \tag{33.15}$$

The specific form of H is not known other than that it results in the human muscle force on the exoskeleton. Figure 33.14 represents the closed-loop system behavior when pilot dynamics is added to the block diagram of Fig. 33.13. Examining Fig. 33.14 reveals that (33.13), representing the new exoskeleton sensitivity function, is not affected by the feedback loop containing H.

Figure 33.14 shows an important characteristic of exoskeleton control. One can observe two feedback loops in the system. The upper feedback loop represents

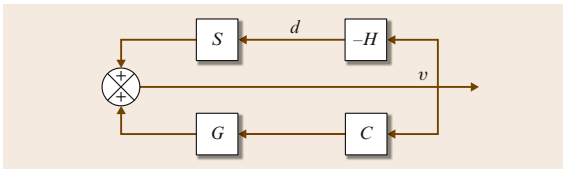

Fig. 33.14 Block diagram showing how an exoskeleton moves. The *upper loop* shows how the pilot moves the exoskeleton through applied forces. The *lower loop* shows how the controller drives the exoskeleton

how forces and torques from the pilot affect the exoskeleton. The lower loop shows how the controlled feedback loop affects the exoskeleton. While the lower feedback loop is positive (potentially destabilizing), the upper feedback loop stabilizes the overall system of pilot and exoskeleton taken as a whole. See [33.38] for detailed stability analysis where it can be seen that, unlike control methods utilized in the control of upper-extremity exoskeletons [33.19], the human dynamics in the control method described here has little potential to destabilize the system. Even though the feedback loop containing C is positive, the feedback loop containing H stabilizes the overall system of pilot and exoskeleton.

The above discussion motivated the design philosophy using a 1-DOF system. An exoskeleton, as shown is a system with many degrees of freedom and therefore implementation of the controller needs further attention. Below we extend the above control technique to the single support phase only. Refer to [33.38] and [33.39] for more details associated with multivariable control.

In the single support phase, the exoskeleton system is modeled as the seven-DOF serial link mechanism in the sagittal plane shown in Fig. 33.15. The inverse dynamics of the exoskeleton can be written in the general form as:

$$M(\theta)\ddot{\theta} + C(\theta,\dot{\theta})\dot{\theta} + P(\theta) = T + d\,,$$
$$\text{where } \theta = (\theta_1\theta_2\ldots\theta_7)^\top \text{ and } T = (0, T_1T_2\ldots T_6)^\top\,. \tag{33.16}$$

M is a 7×7 inertia matrix and is a function of θ, $C(\theta,\dot{\theta})$ is a 7×7 centripetal and Coriolis matrix and is a function of θ and $\dot{\theta}$, and P is a 7×1 vector of gravitational torques and is a function of θ only. T is the 7×1 actuator torque vector with its first element set to zero since there is no actuator associated with joint angle θ_1 (i. e., angle between the exoskeleton foot and the ground); d is the effective 7×1 torque vector imposed by the pilot on the exoskeleton at various locations. According to (33.14), we choose the controller to be the exoskeleton inverse dynamics scaled by $(1-\alpha^{-1})$, where α is

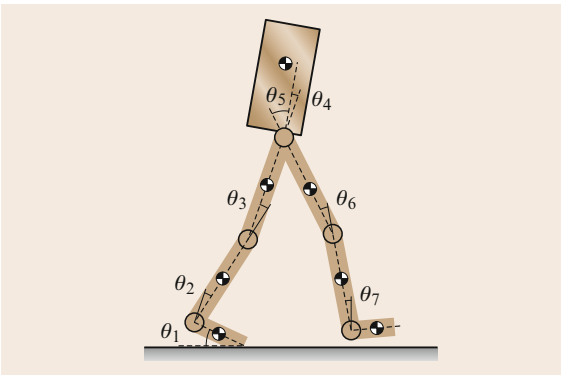

Fig. 33.15 Sagittal plane representation of the exoskeleton in the single stance phase. The *torso* includes the combined exoskeleton torso mechanism, payload, control computer, and power source

the amplification number

$$T = \hat{P} + (1-\alpha^1)[\hat{M}(\theta)\ddot{\theta} + \hat{C}(\theta,\dot{\theta})\dot{\theta}]\,, \tag{33.17}$$

$\hat{C}(\theta,\dot{\theta})$, $\hat{P}(\theta)$ and $\hat{M}(\theta)$ are the estimates of the Coriolis matrix, gravity vector, and the inertia matrix, respectively, for the system shown in Fig. 33.15. Note that (33.17) results in a 7×1 actuator torque. Since there is no actuator between the exoskeleton foot and the ground, the torque prescribed by the first element of T must be provided by the pilot. Substituting T from (33.17) into (33.16) yields,

$$M(\theta)\ddot{\theta} + C(\theta,\dot{\theta})\dot{\theta} + P(\theta)$$
$$= \hat{P}(\theta) + (1-\alpha^{-1})[\hat{M}(\theta)\ddot{\theta} + \hat{C}(\theta,\dot{\theta})\dot{\theta}] + d\,. \tag{33.18}$$

In the limit when $M(\theta) = \hat{M}(\theta)$, $C(\theta,\dot{\theta}) = \hat{C}(\theta,\dot{\theta})$, $P(\theta) = \hat{P}(\theta)$, and α are sufficiently large, d will approach zero, meaning the pilot can walk as if the exoskeleton did not exist. However, it can be seen from (33.18) that the force felt by the pilot is a function of α and the accuracy of the estimates $\hat{C}(\theta,\dot{\theta})$, $\hat{P}(\theta)$, and $\hat{M}(\theta)$. In general, the more accurately the system is modeled, the less the human force, d, will be. In the presence of variations in abduction–adduction angles, only $P(\theta)$ in (33.16) and (33.17) needs to be modified.

Exoskeleton systems use multivariable nonlinear algorithm to robustly control their behavior. Since all computations required to implement the control are conducted on a single computer, one needs a control platform to minimize the number of signal wires in the system. See [33.40] and [33.41] for a novel control platform.

33.8 Highlights of the Lower-Extremity Design

In designing an exoskeleton, several factors had to be considered: Firstly, the exoskeleton needed to exist in the same workspace of the pilot without interfering with his motion. Secondly, it had to be decided whether the exoskeleton should be anthropomorphic (i. e., kinematically matching), or non-anthropomorphic (i. e., kinematically matching the operator only at the connection points between human and machine). Berkeley ultimately selected the anthropomorphic architecture because of its transparency to the pilot. It is also concluded that an exoskeleton that kinematically matches the wearer's legs gains the most psychological acceptance by the user and is therefore safer to wear. Consequently, the exoskeleton was designed to have the same degrees of freedom as the pilot: three degrees at the ankle and the hip, and one degree at the knee. This architecture also allowed the appropriately scaled clinical human walking data to be employed for the design of the exoskeleton components, including the workspace, actuators, and the power source.

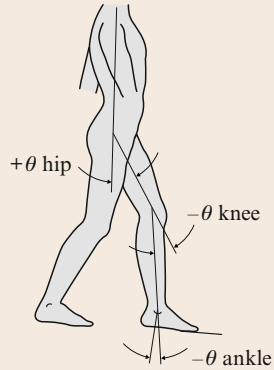

Fig. 33.16 Each joint angle is measured as the positive counterclockwise displacement of the distal link from the proximal link (zero in standing position) with the person oriented as shown. In the position shown, the hip angle is positive whereas both the knee and ankle angles are negative. Torque is measured as positive acting counterclockwise on the distal link

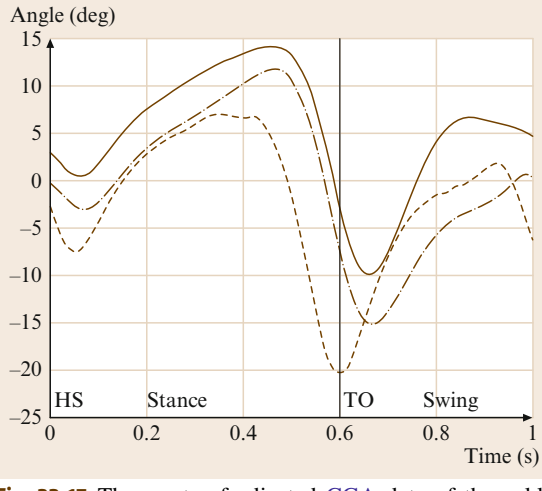

Fig. 33.17 Three sets of adjusted CGA data of the ankle flexion/extension angle. The minimum angle (extension) is $\approx -20°$ and occurs just after toe-off. The maximum angle (flexion) is $\approx +15°$ and occurs in late stance phase

A study of clinical gait analysis (CGA) data provides evidence that humans expend the most power through the sagittal plane joints of the ankle, knee, and hip while walking, squatting, climbing stairs, and most other common maneuvers. For this reason, the sagittal-plane joints of the first prototype exoskeleton are powered. However, to save energy, the nonsagittal degrees of freedom at the ankle and hip remain unpowered. This compels the pilot to provide the force to maneuver the exoskeleton abduction and rotation, where the required operational forces are smaller. To reduce the burden on the human operator further, the unactuated degrees of freedom are spring loaded to a neutral standing position.

Human joint angles and torques for a typical walking cycle were obtained in the form of independently collected CGA data. CGA angle data is typically collected via human video motion capture. CGA torque data is calculated by estimating limb masses and inertias and applying dynamic equations to the motion data. Given the variations in individual gait and measuring methods, three independent sources of CGA data [33.42–44] were utilized for the analysis and design of BLEEX. This data was modified to yield estimates of exoskeleton actuation requirements. The modifications included: (1) scaling the joint torques to a 75 kg person (the projected weight of the exoskeleton and its payload not including its pilot); (2) scaling the data to represent the walking speed of one cycle per second (or about 1.3 m/s); and (3) adding the pelvic tilt angle (or lower back angle depending on data available) to the hip angle to yield a single hip angle between the torso and the thigh, as shown in Fig. 33.16. This accounts for the reduced degrees of freedom of the exoskeleton. The following sections describe the use of CGA data and its implication for the exoskeleton design. The sign conventions used are shown in Fig. 33.16.

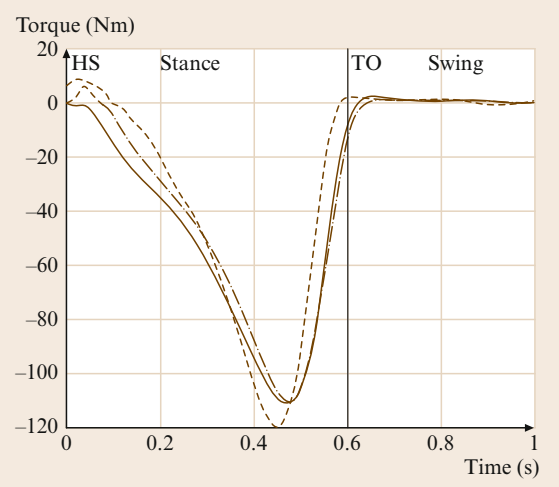

Fig. 33.18 Three sets of adjusted CGA data of the ankle flexion/extension torque. Peak negative torque (extension of the foot) is very large (≈ -120 Nm) and occurs in late stance phase. The ankle torque during swing is quite small

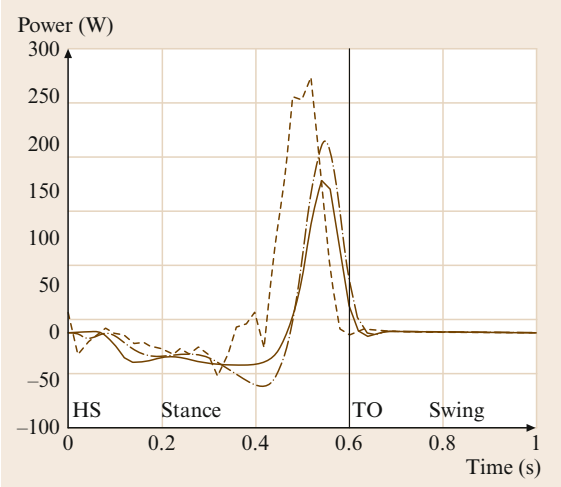

Fig. 33.19 Three sets of adjusted CGA data of the ankle flexion/extension instantaneous mechanical power. The average ankle power is positive, indicating that the ankle does positive work and requires actuation

Figure 33.17 shows the CGA ankle angle data for a 75 kg human walking on flat ground at approximately 1.3 m/s versus time. Although Fig. 33.17 shows a small range of motion while walking (approximately $-20°$ to $+15°$), greater ranges of motion are required for other movements. An average person can flex their ankles anywhere from $-38°$ to $+35°$. The exoskeleton ankle was chosen to have a maximum flexibility of $\pm 45°$ to compensate for the lack of several smaller degrees of freedom in the exoskeleton foot. Through all plots, TO stands for *toe-off* and HS stands for *heel-strike*.

Figure 33.18 shows the adjusted CGA data of the ankle flexion/extension torque. The ankle torque is almost entirely negative, making unidirectional actuators an ideal actuation choice. This asymmetry also implies a preferred mounting orientation for asymmetric actuators (one sided hydraulic cylinders). Conversely, if symmetric bidirectional actuators are considered, spring loading would allow the use of low-torque-producing actuators. Although the ankle torque is large during stance, it is negligible during swing. This suggests a system that disengages the ankle actuators from the exoskeleton during swing to save power.

The instantaneous ankle mechanical power (shown in Fig. 33.19) is calculated by multiplying the joint angular velocity (derived from Fig. 33.17) and the instantaneous joint torque (Fig. 33.18). The ankle absorbs energy during the first half of the stance phase and releases energy just before toe off. The average ankle power is positive, indicating that power production is required at the ankle.

Similar analyses were carried out for the knee and the hip [33.45] and [33.46]. The required knee torque has both positive and negative components, indicating the need for a bidirectional actuator. The highest peak torque is extension in early stance (≈ 60 Nm); hence asymmetric actuators should be biased to provide greater extension torque. The hip torque is relatively symmetric (-80 to $+60$ Nm); hence a bidirectional hip actuator is required. Negative extension torque is required in early stance as the hip supports the load on the stance leg.

Hip torque is positive in late stance and early swing as the hip propels the leg forward during swing. In late swing, the torque goes negative as the hip decelerates the leg prior to heel strike.

CGA data, which provided torque and speed information at each joint of a 75 kg person, was also used to size the exoskeleton power source. The information suggested that a typical person uses about 0.25 HP (185 W) to walk at an average speed of 3 mph. This figure, which represents the average product of speed and torque, is an expression of the purely mechanical power exhibited at the legs during walking. Since it is assumed that the exoskeleton is similar to a human in terms of geometry and weight, one of the key design objectives turned out to be designing a power unit and actuation system to deliver about 0.25 HP at the exoskeleton joints.

Table 33.1 BLEEX joint ranges of motion

	Human walking maximum (*degrees*)	BLEEX maximum (*degrees*)	Average military male maximum (*degrees*)
Ankle flexion	14.1	45	35
Ankle extension	20.6	45	38
Ankle abduction	not available	20	23
Ankle adduction	not available	20	24
Knee flexion	73.5	121	159
Hip flexion	32.2	121	125
Hip extension	22.5	10	not available
Hip abduction	7.9	16	53
Hip adduction	6.4	16	31
Total rotation external	13.2	35	73
Total rotation internal	1.6	35	66

The BLEEX kinematics are close to human leg kinematics, so the BLEEX joint ranges of motion are determined by examining human joint ranges of motion. At the very least, the BLEEX joint range of motion should be equal to the human range of motion during walking (shown in column 1 in Table 33.1), which can be found by examining CGA data [33.42–44]. Safety dictates that the BLEEX range of motion should not be more than the operator's range of motion (shown in column 3 of Table 33.1). For each degree of freedom, the second column of Table 33.1 lists the BLEEX range of motion which is in general larger than the human range of motion during walking and less than the maximum range of human motion.

The most maneuverable exoskeleton should ideally have ranges of motion slightly less than the human's maximum range of motion. However, BLEEX uses linear actuators, so some of the joint ranges of motion are reduced to prevent the actuators' axes of motion from passing through the joint center. If this had not been prevented, the joint could reach a configuration where the actuator would be unable to produce a torque about its joint. Additionally, all the joint ranges of motion were tested and revised during prototype testing. For example, mockup testing determined that the BLEEX ankle flexion/extension range of motion needs to be greater than the human ankle range of motion to accommodate the human foot's smaller degrees of freedom not modeled in the BLEEX foot.

It is natural to design a 3-DOF exoskeleton hip joint such that all three axes of rotation pass through the human ball-and-socket hip joint. However, through the design of several mockups and experiments, we learned that these designs have limited ranges of motion and result in singularities at some human hip postures. Therefore the rotation joint was moved so it does not align with the human's hip joint. Initially the rotation joint was placed directly above each exoskeleton leg (labeled 'alternate rotation' in Fig. 33.20). This worked well for the lightweight plastic mockup, but created problems in the full-scale prototype because the high mass of the torso and payload created a large moment about the unactuated rotation joint. Therefore, the current hip rotation joint for both legs was chosen to be a single axis of rotation directly behind the person and under the torso (labeled 'current rotation' in Fig. 33.20). The current rotation joint is typically spring loaded towards its illustrated position using sheets of spring steel.

Like the human's ankle, the BLEEX ankle has three DOFs. The flexion/extension axis coincides with the human ankle joint. For design simplification, the abduction/adduction and rotation axes on the BLEEX ankle do not pass through the human's leg and form a plane outside of the human's foot (Fig. 33.21). To take load

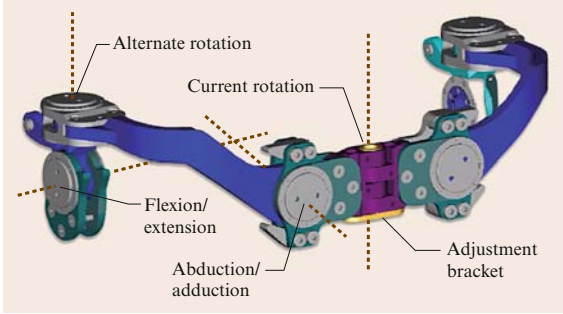

Fig. 33.20 The exoskeleton hip degrees of freedom (back view). Only the rotation axis does not pass through the human hip ball and socket joint. The adjustment bracket is replaceable to accommodate various sized operators

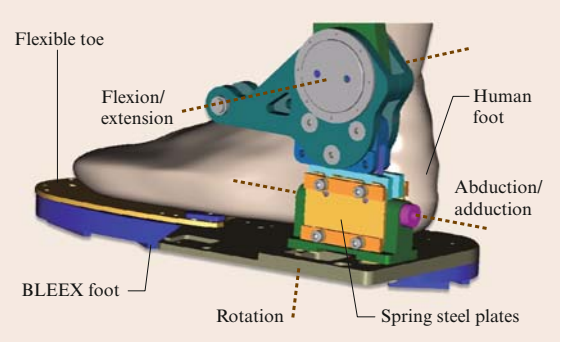

Fig. 33.21 The exoskeleton ankle degrees of freedom. Only the flexion/extension axis passes through the human's ankle joint. Abduction/adduction and rotation axes are not powered, but are equipped with appropriate impedances

off of the human's ankle, the BLEEX ankle abduction/adduction joint is sprung towards vertical, but the rotation joint is completely free. Additionally, the front of the exoskeleton foot, under the operator's toes, is compliant to allow the exoskeleton foot to flex with the human's foot. Since the human and exoskeleton leg kinematics are not exactly the same (merely similar), the human and exoskeleton are only rigidly connected at the extremities (feet and torso).

The BLEEX foot is a critical component due to its variety of functions.

- It measures the location of the foot's center of pressure and therefore identifies the foot's configuration on the ground. This information is necessary for BLEEX control.
- It measures the human's load distribution (how much of the human's weight is on each leg), which is also used in BLEEX control.

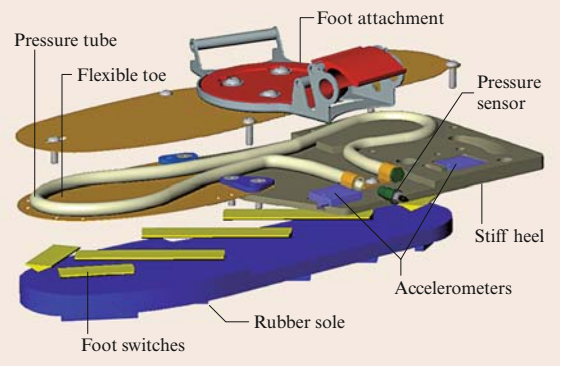

Fig. 33.22 BLEEX foot design (exploded view)

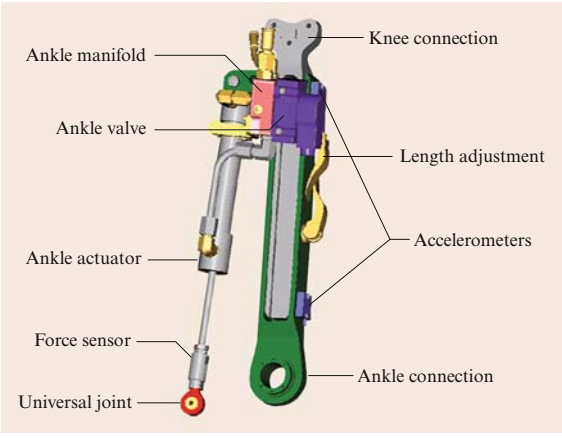

Fig. 33.23 BLEEX shank design

- It transfers BLEEX's weight to the ground, so it must have structural integrity and exhibit long life in the presence of periodic environmental forces.
- It is one of two places where the human and exoskeleton are rigidly connected, so it must be comfortable for the operator.

As shown in Fig. 33.21, the main structure of the foot has a stiff heel to transfer the load to the ground and a flexible toe for comfort. The operator's boot rigidly attaches to the top of the exoskeleton foot via a quick-release binding. Along the bottom of the foot, switches detect which parts of the foot are in contact with the ground. For ruggedness, these switches are molded into a custom rubber sole. Also illustrated in Fig. 33.21 is the load distribution sensor, a rubber *pressure tube* filled with hydraulic oil and sandwiched between the human's

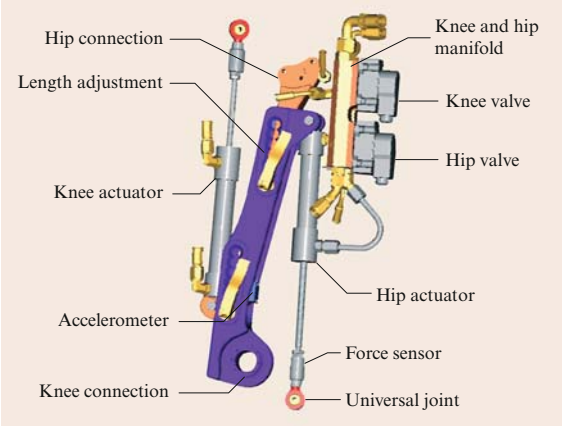

Fig. 33.24 BLEEX thigh design

foot and the main exoskeleton foot structure. Only the weight of the human (not the exoskeleton) is transferred onto the pressure tube and measured by the sensor. This sensor is used by the control algorithm to detect how much weight the human places on their left leg versus their right leg.

The main function of the BLEEX shank and thigh are for structural support and to connect the flexion/extension joints together (Figs. 33.23 and 33.24). Both the shank and thigh are designed to adjust to fit 90% of the population; they consist of two pieces that slide within each other and then lock at the desired length. To minimize the hydraulic routing, manifolds were designed to route the fluid between the valves, actuators, supply, and return lines. These manifolds mount directly to the cylinders to reduce the hydraulic distance between the valves and actuator, maximizing the actuator's performance. The actuator, manifold, and valve for the ankle mount to the shank, while the actuators, manifold, and valves for the knee and hip are on the thigh. One manifold, mounted on the knee actuator, routes the hydraulic fluid for the knee and hip actuators.

Shown in Fig. 33.26, the BLEEX torso connects to the hip structure (shown in Fig. 33.20). The power supply [33.47–49], controlling computer, and payload mount to the rear side of the torso. An inclinometer mounted to the torso gives the absolute angle reference for the control algorithm. A custom harness (Fig. 33.27) mounts to the front of the torso to hold the exoskeleton to the operator. Besides the feet, the harness is the only other location where the user and exoskeleton are rigidly connected. Figure 33.26 also illustrates the actuator, valve, and manifold for the hip abduction/adduction joint.

33.9 Field-Ready Exoskeleton Systems

This section describes two field-ready exoskeletons developed by members of Berkeley Bionics in conjunction with researchers from the University of California.

33.9.1 The ExoHiker Exoskeleton

The ExoHiker exoskeleton (shown in Fig. 33.25) was the first exoskeleton created by the team of Berkeley Bionics and the University of California, and was the first human exoskeleton in the world capable of rigorous customer evaluations as a load-carrying device. It was designed for carrying heavy backpacks for long missions with small changes in altitude. It weighs only 14.5 kg including a power unit and onboard computer. Its payload capacity is 90 kg while the wearer feels negligible load. The noise from this device is imperceptible. A production version of such an exoskeleton would be capable of traveling 68 km with 0.5 kg of batteries (lithium polymer) at an average speed 4.0 km/h while carrying a 68 kg backpack. When supplemented with a small solar panel, its mission time could be unlimited. The ExoHiker is adjustable to fit individuals ranging in height from approximately 1.65 m to 1.91 m tall. All control adjustments can be accessed by the user through a simple handheld liquid-crystal display (LCD) controller equipped with a graphical user interface menu system. This exoskeleton has been evaluated by the Special Operations Research Support Element on trails in the Rocky Mountains, and in the laboratory environment of the Natick Soldier Systems Center.

Fig. 33.25 The ExoHiker™ field-ready exoskeleton is suitable for small slopes and can carry a load of 90 kg (courtesy of Berkeley Bionics, Jan 2005)

Fig. 33.28 The ExoClimber™ field-ready exoskeleton is suitable for rapid ascent of stairs and steep slopes (courtesy of Berkeley Bionics, Oct 2005)

33.9.2 The ExoClimber Exoskeleton

This exoskeleton (shown in Fig. 33.28) is designed to allow rapid ascent of stairs and steep slopes while providing the same long term load carrying capability of ExoHiker. It weighs 23 kg including power source and onboard computer while its payload capacity is 90 kg. This exoskeleton is as loud as an office printer. Its battery requirements are the same as ExoHiker in all situations except ascending steep slopes. During a steep ascent, the ExoClimber is capable of ascending 300 m per 0.5 kg of battery added to the system (while carrying a 68 kg backpack). This exoskeleton has been evaluated by the Special Operations Research Support Element on trails in the Rocky Mountains, and in the laboratory environment of the Natick Soldier Systems Center. The evaluation included hiking on snow with and without snow shoes. The resulting report was extremely favorable, and during one experiment the distance an operator could walk with a 45 kg pack was increased by 900% using the ExoClimber.

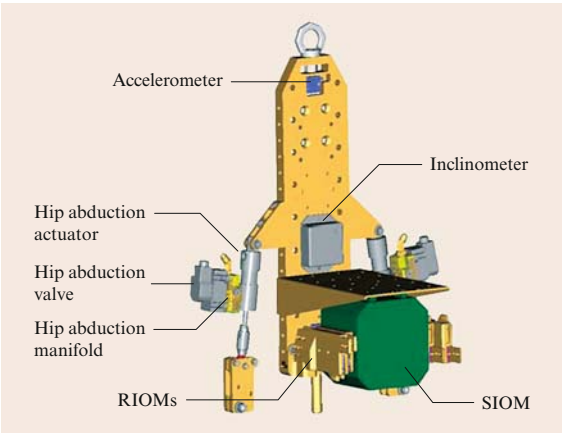

Fig. 33.26 BLEEX torso design (back view)

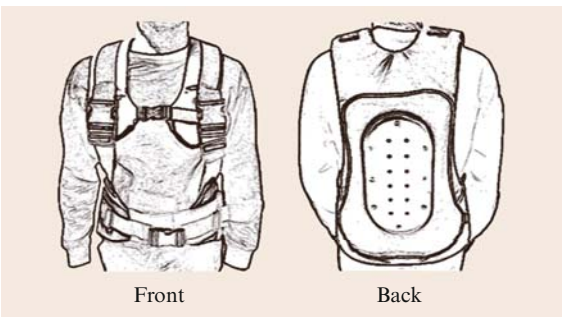

Fig. 33.27 The pilot vests in Fig. 33.10 are designed to distribute the BLEEX–pilot force uniformly on the pilot's upper body

The recent exoskeleton system from Berkeley Bionics now has two independent characteristics: (1) it increases its wearer's maximal load carrying capacity (68 kg to 90 kg), and (2) it decreases its wearer's metabolic cost. During some preliminary evaluations in late 2006 and early 2007, the oxygen consumption of the users walking at a speed of 3.2 km/h, was decreased by 5%–12% when using the latest exoskeleton without a payload. When the users carried a load, the effect was more pronounced. The oxygen consumption of these users carrying a load of 37 kg at a speed of 3.2 km/h was decreased by about 15% when using this exoskeleton. This is the very first exoskeleton in the world that has demonstrated a decrease in oxygen consumption of the user.

33.10 Conclusion and Further Reading

Exoskeleton technology is in its infancy. Although the exoskeleton systems in this analysis are generally considered robotics system worn by humans to carry loads, the reader should be aware that the field of medical orthotics also offers a wealth of knowledge and awareness associated with systems collaborating with patients either as rehabilitation devices or assist devices. For examples of such systems, we invite the readers to see references [33.50, 51] associated with pneumatic ankle orthoses for rehabilitation. At this time, the most limiting issue in exoskeleton technology is the power supply and actuators. Without a viable power supply, exoskeleton systems will be limited to indoor applications.

References

33.1 N.J. Mizen: Preliminary design for the shoulders and arms of a powered, exoskeletal structure, Cornell Aeronaut. Lab. Rep. VO-1692-V-4 (1965)

33.2 General Electric Co.: Hardiman I Arm Test, General Electric Rep. S-70-1019, Schenectady (1969)

33.3 General Electric Co.: Hardiman I Prototype Project, Special Interim Study, General Electric Rep. S-68-1060, Schenectady (1968)

33.4 P.F. Groshaw, General Electric Co.: Hardiman I Arm Test, Hardiman I Prototype, General Electric Rep. S-70-1019, Schenectady (1969)

33.5 B.J. Makinson, General Electric Co.: Research and Development Prototype for Machine Augmentation of Human Strength and Endurance, Hardiman I Project, General Electric Rep. S-71-1056, Schenectady (1971)

33.6 R.S. Mosher: Force-reflecting electrohydraulic manipulator, Electro-Technology (1960)

33.7 M. Vukobratovic, V. Ciric, D. Hristic: Controbution to the Study of Active Exosksltons, Proc. Of the 5th IFAC Congress (Paris, 1972)

33.8 D. Hristic, M. Vukobratovic: Development of active aids for handicapped, Proc. III International Conference on _bio-Mediacl Engineering (Sorrento, 1973)

33.9 A. Seireg, J. Grundmann: *Design of a Multitask Exoskeletal Walking Device for Paraplegics*, *Biomechanics of Medical Devices* (Marcel Dekker, New York 1981) pp. 569–644

33.10 K. Yamamoto, K. Hyodo, M. Ishii, T. Matsuo: Development of power assisting suit for assisting nurse labor, JSME Int. J. Ser. C **45**(3), 703–711 (2002)

33.11 K. Yamamoto, M. Ishii, K. Hyodo, T. Yoshimitsu, T. Matsuo: Development of Power assisting suit, JSME Int. J. Ser. C **46**(3), 923–930 (2003)

33.12 J.E. Pratt, B.T. Krupp, C.J. Morse, S.H. Collins: The RoboKnee: An Exoskeleton for Enhancing Strength and Endurance During Walking, Proc. IEEE International Conference on Robotics and Automation (New Orleans, 2004) pp. 2430–2435

33.13 H. Kawamoto, Y. Sankai: Power assist system HAL-3 for gait disorder person, Int. Conf. Computer Helping People with Special Needs (Linz, 2002)

33.14 H. Kawamoto, S. Kanbe, Y. Sankai: Power assist method for HAL-3 estimating operator's intention based on motion information, Proc. of 2003 IEEE Workshop on Robot and Human Interactive Communication (Millbrae, 2003) pp. 67–72

33.15 K. Kong, D. Jeon: Design and control of an exoskeleton for the elderly and patients, IEEE/ASME Trans. Mechatron. **11**(4), 220–226 (2006)

33.16 S.K. Agrawal, A. Fattah: Theory and design of an orthotic device for full or partial gravity-balancing of a human leg during motion, IEEE Trans. Neural Syst. Rehab. Eng. **12**(2), 157–165 (2004)

33.17 H. Kazerooni, S. Mahoney: Dynamics and control of robotic systems worn by humans, ASME J. Dyn. Syst. Meas. Contr. **113**(3), 379–387 (1991)

33.18 H. Kazerooni, M. Her: The dynamics and control of a haptic interface device, IEEE Trans. Robot. Autom. **10**(4), 453–464 (1994)

33.19 H. Kazerooni, T. Snyder: A case study on dynamics of haptic devices: Human induced instability in powered hand controllers, AIAA J. Guid. Contr. Dyn. **18**(1), 108–113 (1995)

33.20 H. Kazerooni: Human-robot interaction via the transfer of power and information signals, IEEE Trans. Syst. Cybernet. **20**(2), 450–463 (1990)

33.21 H. Kazerooni, J. Guo: Human extenders, ASME J. Dyn. Syst. Meas. Contr. **115**(2B), 281–289 (1993)

33.22 H. Kazerooni: The extender technology at the University of California Berkeley, J. Soc. Instrum. Control Eng. Jpn. **34**, 291–298 (1995)

33.23 H. Kazerooni: The human power amplifier technology at the University of California Berkeley, J. Robot. Auton. Syst. **19**, 179–187 (1996)

33.24 U. Yutaka, H. Kazerooni: A μ-based synthesis based control for compliant maneuver, IEEE Conference on Systems, Man, and Cybernetics (Tokyo, 1999) pp. 1014–1019

33.25 T.J. Snyder, H. Kazerooni: A novel material handling system, IEEE International Conference on Robotics and Automation (1996) pp. 1147–1152

33.26 H. Kazerooni, T.B. Sheridan, P.K. Houpt: Robust compliant motion for manipulators, Part I: The

fundamental concepts of compliant motion, IEEE J. Robot. Autom. **2**(2), 83–92 (1986)
33.27 H. Kazerooni: On the robot compliant motion control, ASME J. Dyn. Syst. Meas. Contr. **111**(3), 416–425 (1989)
33.28 H. Kazerooni, B.J. Waibel, S. Kim: On the stability of robot compliant motion control: Theory and experiments, ASME J. Dyn. Syst. Meas. Contr. **112**(3), 417–426 (1990)
33.29 H. Kazerooni, B.J. Waibel: Theories and experiments on the stability of robot compliance control, IEEE Trans. Robot. Autom. **7**(1), 95–104 (1991)
33.30 Pneumatic human power amplifier module, Patent #5,915,673
33.31 Human power amplifier for vertical maneuvers (U.S. Patent #5,865,426)
33.32 Human power amplifier for lifting load with slack prevention apparatus (U.S. Patent #6,622,990)
33.33 Device and Method for Wireless Lifting Assist Device (U.S. Patent #6,681,638)
33.34 H. Kazerooni, D. Fairbanks, A. Chen, G. Shin: The Magic Glove, IEEE International Conference on Robotics and Automation (New Orleans, 2004)
33.35 H. Kazerooni, C. Foley: A practical robotic end-effector for grasping postal sacks, ASME J. Dyn. Syst. Meas. Contr. **126**, 154–161 (2004)
33.36 H. Kazerooni, C. Foley: A robotic mechanism for grasping sacks, IEEE Trans. Autom. Sci. Eng. **2**(2), 111–120 (2005)
33.37 J. Ghan, R. Steger, H. Kazerooni: Control and system identification for the Berkeley lower extremity exoskeleton, Adv. Robot. **20**(9), 989–1014 (2006)
33.38 H. Kazerooni, R. Steger: The Berkeley lower extremity exoskeletons, ASME J. Dyn. Syst. Meas. Contr. **128**, 14–25 (2006)
33.39 H. Kazerooni, L. Huang, J.L. Racine, R. Steger: On the Control of Berkeley Lower Extremity Exoskeleton (BLEEX), Proc. of IEEE International Conference on Robotics and Automation (Barcelona, 2005)
33.40 S. Kim, G. Anwar, H. Kazerooni: High-speed Communication Network for Controls with Application on the Exoskeleton, American Control Conference (Boston, 2004)
33.41 S. Kim, H. Kazerooni: High Speed Ring-based distributed Networked control system For Real-Time Multivariable Applications, ASME International Mechanical Engineering Congress (Anaheim, 2004)
33.42 C. Kirtley: CGA Normative Gait Database, Hong Kong Polytechnic University. (available http://guardian.curtin.edu.au/cga/data/)
33.43 A. Winter: International Society of Biomechanics, Biomechanical Data Resources, Gait Data. (available http://www.isbweb.org/data/)
33.44 J. Linskell: CGA Normative Gait Database, Limb Fitting Centre, Dundee, Scotland, Young Adult. (available http://guardian.curtin.edu.au/cga/data/)
33.45 A. Chu, H. Kazerooni, A. Zoss: On the Biomimetic Design of the Berkeley Lower Extremity Exoskeleton (BLEEX), Proc. of IEEE International Conference on Robotics and Automation (Barcelona, 2005)
33.46 A. Zoss, H. Kazerooni, A. Chu: On the biomechanical design of the Berkeley lower extremity exoskeleton (BLEEX), IEEE/ASME Trans. Mechatron. **11**(2), 128–138 (2006)
33.47 T. McGee, J. Raade, H. Kazerooni: Monopropellant-driven free piston hydraulic pump for mobile robotic systems, J. Dyn. Syst. Meas. Contr. **126**, 75–81 (2004)
33.48 J. Raade, H. Kazerooni, T. McGee: Analysis and design of a novel power supply for mobile robots, IEEE Trans. Autom. Sci. Eng. **2**(3), 226–232 (2005)
33.49 K. Amundson, J. Raade, N. Harding, H. Kazerooni: Hybrid Hydraulic-Electric Power Unit for Field and Service Robots, Proc. of IEEE Intelligent Robots and Systems (Edmonton, 2005)
33.50 D.P. Ferris, V. Czerniecki, B. Hannaford: An ankle-foot orthosis powered by artificial muscles, J. Appl. Biomech. **21**, 189–197 (2005)
33.51 D.P. Ferris, K.E. Gordon, G.S. Sawicki, A. Peethambaran: An improved powered ankle-foot orthosis using proportional myoelectric control, Gait Posture **23**, 425–428 (2006)